7. Biological Oscillators and Switches

7.1 Motivation, Brief History and Background

Although living biological systems are immensely complex, they are at the same time highly ordered and compactly put together in a remarkably efficient way. Such systems concisely store the information and means of generating the mechanisms required for repetitive cellular reproduction, organisation, control and so on. To see how efficient they can be you need only compare the information storage efficiency per weight of the most advanced computer chip with, say, the ribonucleic acid molecule (mRNA) or a host of others: we are talking here of factors of the order of billions. This chapter, and the next two, are mainly concerned with oscillatory processes. In the biomedical sciences these are common, appear in widely varying contexts and can have periods from a few seconds to hours to days and even weeks. We consider some in detail in this chapter, but mention here a few others from the large number of areas of current research involving biological oscillators.

The periodic pacemaker in the heart is, of course, an important example, which is touched on in Chapter 9. The book by Keener and Sneyd (1998) dicsusses this aspect at length: it is an excellent introduction to mathematical models in physiology in general, covering a wide spectrum of topics. The approximately 24-hour periodic emergence of fruit flies from their pupae might appear to be governed by the external daily rhythm, but this is not the case; see the elegant books by Winfree (1987, 2000) for a detailed exposition of biological clocks and biological time in general. We briefly discuss this fruit fly phenomenon in Chapter 9. There is the now classical work of Hodgkin and Huxley (1952) on nerve action potentials, which are the electrical impulses which propagate along a nerve fibre. This is now a highly developed mathematical biology area (see, for example, the review article by Rinzel 1981 and the book by Keener and Sneyd 1998). Under certain circumstances such nerve fibres exhibit regular periodic firing. The propagation of impulses in neurons normally relies on a threshold stimulus being applied, and is an important practical example of an excitable medium. We discuss a major model for the regular periodic firing behaviour and threshold behaviour in Section 7.5 below and its application to the wave phenomena in Chapter 1, Volume II.

Breathing is a prime example of another physiological oscillator, here the period is of the order of a second. There are many others, such as certain neural activity in the brain, where the cycles have very small periods. A different kind of oscillator is that observed in the glycolytic pathway. Glycolysis is the process that breaks down glucose to provide the energy for cellular metabolism; oscillations with periods of several min-

utes are observed in the concentrations of certain chemicals in the process. The book on biochemical oscillations and cellular rhythms by Goldbeter (1996) gives a thorough and extensive discussion of this as well as other phenomena; he also discusses the molecular basis for chaotic behaviour. Blood testosterone levels in man are often observed to oscillate with periods of the order of 2–3 hours. In Section 7.6 we discuss the modelling of this physiological process and relate it to the practice of chemical castration for a variety of reasons, one of which is to control the growth of prostate tumours. This model is also related to recent work on a male contraceptive pill.

At certain stages in the life cycle of the cellular slime mould, *Dictyostelium discoideum*, the cells emit the chemical cyclic-AMP periodically, with a period of a few minutes. This important topic has been extensively studied theoretically and experimentally; see, for example, the relevant chapter on the periodic aspects in Segel (1984), the models proposed by Martiel and Goldbeter (1987), Monk and Othmer (1989) and the book by Goldbeter (1996). Othmer and Schaap (1999) give an extensive review which covers the major aspects of this important area of signal transduction and the properties of this slime mould in general. Wave phenomena associated with this slime mould are also rich in structure as we shall show in Chapter 1, Volume II; the review by Othmer and Schaap (1999) particularly deals with such spatial wave phenomena. The process of regular cell division in *Dictyostelium*, where the period is measured in hours, indicates a governing biological oscillator of some kind.

All of the above examples are different to the biological clocks associated with circadian or daily rhythms, which are associated with external periodicities, in that they are more reasonably described as autonomous oscillators. Limit cycle oscillators, of the kind we consider here, must of course be open systems from thermodynamic arguments, but they are *not* periodic by virtue of some external periodic forcing function.

Since the subject of biological oscillators is now so large, it is quite impossible to give a remotely comprehensive coverage of the field here. Instead we concentrate on a few general results and some useful simple models which highlight different concepts; we analyse these in detail. We also discuss some of the areas and mechanisms of practical importance and current interest. A knowledge of these is essential in extending the mathematical modelling ideas to other situations. We have already seen periodic behaviour in population models such as discussed in Chapters 1–3, and, from Chapter 6, that it is possible in enzyme kinetics reactions. Other well-known examples, not yet mentioned, are the more or less periodic outbreaks of a large number of common diseases; we shall briefly touch on these in Chapter 10 and give references there.

The history of oscillating reactions really dates from Lotka (1910) who put forward a theoretical reaction which exhibits damped oscillations. Later Lotka (1920, 1925) proposed the reaction mechanism which now carries the Lotka–Volterra label and which we discussed in its ecological context in Chapter 3 and briefly in its chemical context in the last chapter. Experimentally oscillations were found by Bray (1921) in the hydrogen peroxide–iodate ion reaction where temporal oscillations were observed in the concentrations of iodine and rate of oxygen evolution. He specifically referred to Lotka's early paper. This interesting and important work was dismissed and widely disbelieved since, among other criticisms, it was mistakenly thought that it violated the second law of thermodynamics. It doesn't of course since the oscillations eventually die out, but they only do so slowly.

The next major discovery of an oscillating reaction was made by Belousov (1951, 1959), the study of which was continued by Zhabotinskii (1964) and is now known as the Belousov–Zhabotinskii reaction. This important paradigm reaction is the subject matter of Chapter 8. There are now many reactions which are known to admit periodic behaviour; the book of articles edited by Field and Burger (1985) describes some of the detailed research in the area, in particular that associated with the Belousov–Zhabotinskii reaction. Other areas are treated in the books by Goldbeter (1996) and Keener and Sneyd (1998).

In the rest of this section we comment generally about differential equation systems for oscillators and in the following section we describe some special control mechanisms, models which have proved particularly useful for demonstrating typical and unusual behaviour of oscillators. They are reasonable starting points for modelling real and specific biological phenomena associated with periodic behaviour. Some of the remarks are extensions or generalisations of what we did for two-species systems in Chapters 3 and 6.

The models for oscillators which we are concerned with here, with the exception of that in Section 7.6, all give rise to systems of ordinary differential equations (of the type (3.43) studied in Chapter 3) for the concentration vector $\mathbf{u}(t)$; namely,

$$\frac{d\mathbf{u}}{dt} = \mathbf{f}(\mathbf{u}), \tag{7.1}$$

where $\mathbf{f}$ describes the nonlinear reaction kinetics, or underlying biological oscillator mechanism. The mathematical literature on nonlinear oscillations is large and daunting, but much of it is not of relevance to real biological modelling. Even though quite old, a good practical review from a mathematical biology point of view, is given by Howard (1979). Mostly we are interested here in periodic solutions of (7.1) such that

$$\mathbf{u}(t + T) = \mathbf{u}(t), \tag{7.2}$$

where $T > 0$ is the period. In the phase space of concentrations this solution trajectory is a simple closed orbit, γ say. If $\mathbf{u}_0(t)$ is a limit cycle solution then it is asymptotically stable (globally) if any perturbation from $\mathbf{u}_0$, or γ, eventually tends to zero as $t \to \infty$.

It is always the case with realistic, qualitative as well as quantitative, biological models that the differential equations involve parameters, generically denoted by λ, say. The behaviour of the solutions $\mathbf{u}(t; \lambda)$ varies with the values or ranges of the parameters as we saw, for example, in Chapter 3. Generally steady state solutions of (7.1), that is, solutions of $\mathbf{f}(\mathbf{u}) = 0$, are stable to small perturbations if λ is in a certain range, and become unstable when λ passes through a critical value λ_c, a *bifurcation point*. When the model involves only two dependent variables the analysis of (7.1) can be carried out completely in the phase plane (see Appendix A) as we saw in Chapters 3 and 6. For higher-order systems the theory is certainly not complete and each case usually has to be studied individually. A major exception is provided by the *Hopf bifurcation theorem*, the results for which strictly hold only near the bifurcation values. A basic, useful and easily applied result of the Hopf theorem is the following.

Let us suppose that $\mathbf{u} = 0$ is a steady state of (7.1) and that a linearization about it gives a simple complex conjugate pair of eigenvalues $\alpha(\lambda) = \mathrm{Re}\,\alpha \pm i\,\mathrm{Im}\,\alpha$. Now suppose this pair of eigenvalues has the largest real part of all the eigenvalues and is such that in a small neighbourhood of a bifurcation value λ_c, (i) $\mathrm{Re}\,\alpha < 0$ if $\lambda < \lambda_c$, (ii) $\mathrm{Re}\,\alpha = 0$ and $\mathrm{Im}\,\alpha \neq 0$ if $\lambda = \lambda_c$ and (iii) $\mathrm{Re}\,\alpha > 0$ if $\lambda > \lambda_c$. Then, in a small neighbourhood of λ_c, $\lambda > \lambda_c$ the steady state is unstable by growing oscillations and, at least, a small amplitude *limit cycle periodic solution* exists about $\mathbf{u} = 0$. Furthermore the period of this limit cycle solution is given by $2\pi/T_0$ where $T_0 = \mathrm{Im}\,[\alpha(\lambda_c)]$. The value λ_c is a *Hopf bifurcation* value. The theorem says nothing about the stability of such limit cycle solutions although in practice with real biological systems they usually are when numerically simulated.

7.2 Feedback Control Mechanisms

It is well documented that in a large number of cell cultures some of the enzymes involved show periodic increases in their activity during division, and these reflect periodic changes in the rate of enzyme synthesis; Goldbeter (1996) has some examples of this. The article by Tyson (1979, see also 1983) lists several specific cases where this happens. Regulatory mechanisms require some kind of feedback control. In a classic paper, mainly on regulatory mechanisms in cellular physiology, Monod and Jacob (1961) proposed several models which were capable of self-regulation and control and which are known to exist in bacteria. One of these models suggests that certain metabolites repress the enzymes which are essential for their own synthesis. This is done by inhibiting the transcription of the molecule DNA to messenger RNA (mRNA), which is the template which makes the enzyme. Goodwin (1965) proposed a simple model for this process which is schematically shown in Figure 7.1 in the form analysed in detail by Hastings et al. (1977).

A generalisation of Goodwin's (1965) model which also reflects a version of the process in Figure 7.1 is

$$\begin{aligned} \frac{dM}{dt} &= \frac{V}{D + P^m} - aM, \\ \frac{dE}{dt} &= bM - cE, \\ \frac{dP}{dt} &= dE - eP, \end{aligned} \tag{7.3}$$

where M, E and P represent respectively the concentrations of the mRNA, the enzyme and the product of the reaction of the enzyme and a substrate, assumed to be available at a constant level. All of V, K, m (the Hill coefficient) and a, b, c, d and e are constant positive parameters. Since DNA is externally supplied in this process we do not need an equation for its concentration. With the experience gained from Chapter 6 we interpret this model (7.3) as follows. The creation of M is inhibited by the product P and is degraded according to first-order kinetics, while E and P are created and degraded by first-order kinetics. Clearly more sophisticated kinetics could reasonably be used with

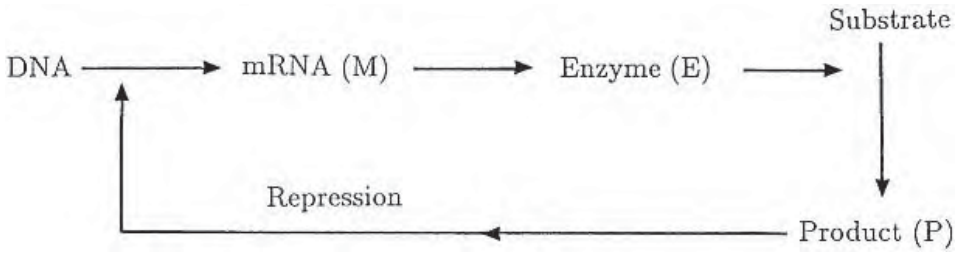

Figure 7.1. Schematic control system for the production of an enzyme (E) according to the model system (7.3). Here, the enzyme combines with the substrate to produce a product (P) which represses the transcription of DNA to mRNA (M), the template for making the enzyme.

the methods described in Chapter 6. By considering the stability of the steady state, Griffith (1968) showed that oscillations are not possible unless the Hill coefficient m in the first of (7.3) is sufficiently large (see Exercise 4), roughly greater than 8—an unnaturally high value. For m in this range the system does exhibit limit cycle oscillations.

A more biologically relevant modification is to replace the P-equation in (7.3) by

$$\frac{dP}{dt} = dE - \frac{eP}{k+P}.$$

That is, degradation of the product saturates for large P according to Michaelis–Menten kinetics. With this in place of the linear form, limit cycle oscillations can occur for low values of the Hill coefficient m, even as low as $m = 2$.

The concept of a sequence of linked reactions is a useful one and various modifications have been suggested. In one, which has been widely used and studied, the number of reactions has been increased generally to n and the feedback function made more more general and hence widely applicable. In a suitable nondimensional form the system is

$$\begin{aligned} \frac{du_1}{dt} &= f(u_n) - k_1 u_1, \\ \frac{du_r}{dt} &= u_{r-1} - k_r u_r, \quad r = 2, 3, \ldots, n, \end{aligned} \tag{7.4}$$

where the $k_r > 0$ and $f(u)$, which is always positive, is the nonlinear feedback function. If $f(u)$ is an increasing function of u, $f'(u) > 0$, (7.4) represents a *positive feedback* loop, while if $f(u)$ is a monotonic decreasing function of u, $f'(u) < 0$, the system represents a *negative feedback* loop or *feedback inhibition*. Positive feedback loops are not common metabolic control mechanisms, whereas negative ones are; see, for example, Tyson and Othmer (1978) and Goldbeter (1996). Yagil and Yagil (1971) suggested specific forms for $f(u)$ for several biochemical situations.

Steady state solutions of (7.4) are given by

$$\begin{aligned} f(u_n) &= k_1 k_2 \ldots k_n u_n, \\ u_{n-1} &= k_n u_n, \ldots, \quad u_1 = k_2 k_3 \ldots k_n u_n \end{aligned} \tag{7.5}$$

the first of which is most easily solved graphically by plotting $f(u)$ and noting the intersections with the straight line $k_1k_2 \ldots k_nu$. With positive feedback functions $f(u)$, multiple steady states are possible whereas with feedback inhibition there is always a unique steady state (see Exercise 3).

Although with higher-dimensional equation systems there is no equivalent of the Poincaré–Bendixson theorem for the two-dimensional phase plane (see Appendix A), realistic systems must have some enclosing domain with boundary B, that is, a confined set, such that

$$\mathbf{n} \cdot \frac{d\mathbf{u}}{dt} < 0 \quad \text{for} \quad \mathbf{u} \text{ on } B, \tag{7.6}$$

where $\mathbf{n}$ is the outward unit normal to B.

In the case of the more important negative feedback systems of the type (7.4), the determination of such a domain is quite simple. As we noted, we are, of course, only interested in nonnegative values for $\mathbf{u}$. Consider first the two-species case of (7.4), namely,

$$\frac{du_1}{dt} = f(u_2) - k_1u_1, \quad \frac{du_2}{dt} = u_1 - k_2u_2,$$

where $f(u_2) > 0$ and $f'(u_2) < 0$. Consider first the rectangular domain bounded by $u_1 = 0$, $u_2 = 0$, $u_1 = U_1$ and $u_2 = U_2$, where U_1 and U_2 are to be determined. On the boundaries

$$\begin{aligned}
&u_1 = 0, \quad \mathbf{n} \cdot \frac{d\mathbf{u}}{dt} = -\frac{du_1}{dt} = -f(u_2) < 0 \quad \text{for all} \quad u_2 \geq 0,\\
&u_2 = 0, \quad \mathbf{n} \cdot \frac{d\mathbf{u}}{dt} = -\frac{du_2}{dt} = -u_1 < 0 \quad \text{for} \quad u_1 > 0,\\
&u_1 = U_1, \quad \mathbf{n} \cdot \frac{d\mathbf{u}}{dt} = f(u_2) - k_1U_1 < 0\\
&\qquad \text{if } U_1 > \frac{f(u_2)}{k_1} \quad \text{for all} \quad 0 \leq u_2 \leq U_2 \quad \Rightarrow \quad U_1 > \frac{f(0)}{k_1}\\
&u_2 = U_2, \quad \mathbf{n} \cdot \frac{d\mathbf{u}}{dt} = u_1 - k_2U_2 < 0\\
&\qquad \text{if } U_2 > \frac{u_1}{k_2} \quad \text{for all} \quad 0 < u_1 \leq U_1.
\end{aligned} \tag{7.7}$$

If we now choose U_1 and U_2 to satisfy the inequalities

$$U_1 > \frac{f(0)}{k_1}, \quad U_2 > \frac{U_1}{k_2} \tag{7.8}$$

then (7.7) shows that there is a confined set B on which (7.6) is satisfied. We can always find such U_1 and U_2 when $f(u)$ is a monotonic decreasing function of u. Note that the positive steady state, given by the unique solution of

$$u_1 = k_2 u_2, \quad f(u_2) = k_1 k_2 u_2$$

always lies inside the domain B defined by (7.7) and (7.8), and, since $f'(u) < 0$, it is always linearly stable, since the eigenvalues of the stability (or community) matrix are both negative. Thus the two-species model cannot admit limit cycle oscillations.

It is now clear how to generalise the method to determine a domain boundary B on which (7.6) is satisfied for an n-species negative feedback loop. The appropriate confined set is given by the box bounded by the planes $u_r = 0$, $r = 1, 2, \ldots, n$ and $u_r = U_r$, $r = 1, 2, \ldots, n$, where any U_r, $r = 1, \ldots, n$ satisfying

$$U_1 > \frac{f(0)}{k_1}, \quad U_2 > \frac{U_1}{k_2}, \ldots, \quad U_n > \frac{U_1}{k_1 k_2 \ldots k_n} \tag{7.9}$$

will suffice. As in the two-species case the steady state always lies inside such a boundary B.

Whether or not such systems with $n \geq 3$ admit periodic solutions is more difficult to determine than in the two-species case (see Exercise 4). As the order of the system goes up the possibility of periodic solutions increases. If we consider the oscillator (7.3) or, in its dimensionless form (7.4) for u_1, u_2, u_3 with $f(u_3) = 1/(1 + u_3)$, it can be shown that the steady state is always stable (Exercise 4). If we have $f(u_3) = 1/(1+u_3^m)$ then (Exercise 4), using the Routh–Hurwitz conditions on the cubic for the eigenvalues of the stability matrix, the steady state is only unstable if $m > 8$, which, as we have mentioned, is an unrealistically high value for the implied cooperativity. As the number of reactions, n, goes up, Tyson and Othmer (1978) have shown that the steady state goes unstable if the cooperativity m and the length of the feedback loop n are such that $m > m_0(n) = \sec^n(\pi/n)$. When $n = 3$ this gives $m = 8$ as above: some values for higher n are $n = 4$, $m = 4$; $n = 10$, $m = 1.65$ and $n \to \infty$, $m \to 1$.

By linearising (7.4) about the steady state (7.5), conditions on the function and parameters can be found such that limit cycle periodic solutions exist: MacDonald (1977), for example, used bifurcation theory while Rapp (1976) developed a numerical search procedure for the full nonlinear system and gave quantitative estimates for the period of oscillation.

We can get some analytical approximations for the period of the solutions, when they exist, using a method suggested by Tyson (1979). First we use a result pointed out by Hunding (1974), namely, that most of the kinetics parameters $k_1, k_2, \ldots, k_n$ must be approximately equal or oscillatory solutions will not be possible for low values of m. To see this, first note that each k_r is associated with the inverse of the dimensionless half-life time of u_r. Suppose, for example, that one of the constants, say k_s, is much larger than all the others, and choose a time t_1 such that $t_1 \gg 1/k_s$ and $t_1 \ll 1/k_r$ for all $r \neq s$. As the system evolves over a time interval $0 \leq t \leq t_1$, since $k_r t_1 \ll 1$ for all $r \neq s$, from (7.4) u_{s-1} does not change much in this time interval. So, the solution of the ordinary differential equation for $u_s(t)$ from (7.4) with u_{s-1} constant, is

$$u_s(t) \approx u_s(0) \exp[-k_s t] + \frac{u_{s-1}}{k_s}\{1 - \exp[-k_s t]\}, \quad 0 \leq t \leq t_1.$$

But, since $k_s t_1 \gg 1$, the last equation gives $u_s(t) \approx u_{s-1}/k_s$ which means that the sth species is essentially at its pseudo-steady state (since $du_s/dt = u_{s-1} - k_s u_s \approx 0$) over the time interval that all the other species change appreciably. This says that the sth species is effectively not involved in the feedback loop process and so the order of the loop is reduced by one to $n - 1$.

Now let K be the smallest of all the kinetics parameters and denote the half-life of u_K by H; this is the longest half-life of all the species. Using the above result, the effective length of the feedback loop is equal to the number N of species whose half-lives are all roughly the same as H or, what is the same thing, have rate constants $k \approx K$. All the other reactions take place on a faster timescale and so are not involved in the reaction scheme.

Suppose now we have a periodic solution and consider one complete oscillation in which each of the species undergoes an increase, then a decrease, to complete the cycle. Start off with u_1 which first increases, then u_2, then u_3 and so on to u_N. Then u_1 decreases, then u_2 and so on until u_N decreases. There is thus a total of $2N$ steps involved in the oscillation with each increase and decrease taking approximately the same characteristic time $1/K$. So, the approximate period T of the oscillation is $T \approx 2N/K$. A more quantitative result for the period has been given by Rapp (1976) who showed that the frequency Ω is given by

$$\Omega = K \tan\left(\frac{\pi}{N}\right) \quad \Rightarrow \quad T = \frac{2\pi}{\Omega},$$

which reduces to $T \approx 2N/K$ for large N.

The dynamic behaviour of the above feedback control circuits, and generalisations of them, in biochemical pathways have been treated in depth by Tyson and Othmer (1978), and from a more mathematical point of view by Hastings et al. (1977). The latter prove useful results for the existence of periodic solutions for systems with more general reactions than the first-order kinetics feedback loops we have just considered.

It is encouraging from a practical point of view that it is very often the case that if (i) a steady state becomes unstable by growing oscillations at some bifurcation value of a parameter, and (ii) there is a confined set enclosing the steady state, then a limit cycle oscillation solution exists. Of course in any specific example it has to be demonstrated, and if possible proved, that this is indeed the case. But, as this can often be difficult to do, it is better to try predicting from experience and heuristic reasoning and then simulate the system numerically rather than wait for a mathematical proof which may not be forthcoming. An unstable steady state with its own confined set (7.6), although necessary, are not sufficient conditions for an oscillatory solution of (7.1) to exist. One particularly useful aspect of the rigorous mathematical treatment of Hastings et al. (1977) is that it gives some general results which can be used on more realistic feedback circuits which better mimic real biochemical feedback control mechanisms.

Tyson (1983) proposed a negative feedback model similar to the above to explain periodic enzyme synthesis. He gives an explanation as to why the period of synthesis is close to the cell cycle time when cells undergo division.

7.3 Oscillators and Switches Involving Two or More Species: General Qualitative Results

We have already seen in Chapter 3 that two-species models of interacting populations can exhibit limit cycle periodic oscillations. Here we derive some general results as regards the qualitative character of the reaction kinetics which may exhibit such periodic solutions.

Let the two species u and v satisfy reaction kinetics given by

$$\frac{du}{dt} = f(u, v), \frac{dv}{dt} = g(u, v), \tag{7.10}$$

where, of course, f and g are nonlinear. Steady state solutions (u_0, v_0) of (7.10) are given by

$$f(u_0, v_0) = g(u_0, v_0) = 0, \tag{7.11}$$

of which only the positive solutions are of interest. Linearising about (u_0, v_0) we have, in the usual way (see Chapter 3),

$$\begin{pmatrix} \dfrac{d(u-u_0)}{dt} \\ \dfrac{d(v-v_0)}{dt} \end{pmatrix} = A \begin{pmatrix} u-u_0 \\ v-v_0 \end{pmatrix}, \quad A = \begin{pmatrix} f_u & f_v \\ g_u & g_v \end{pmatrix}_{u_0, v_0}. \tag{7.12}$$

The linear stability of (u_0, v_0) is determined by the eigenvalues λ of the stability matrix A, given by

$$\begin{aligned} |A - \lambda I| = 0 \quad &\Rightarrow \quad \lambda^2 - (\mathrm{tr}A)\lambda + |A| = 0. \\ &\Rightarrow \quad \lambda = \frac{1}{2}\left\{\mathrm{tr}A \pm [(\mathrm{tr}A)^2 - 4|A|]^{1/2}\right\}. \end{aligned} \tag{7.13}$$

Necessary and sufficient conditions for stability are

$$\mathrm{tr}A = f_u + g_v < 0, \quad |A| = f_u g_v - f_v g_u > 0, \tag{7.14}$$

where here, and in what follows unless stated otherwise, the derivatives are evaluated at the steady state (u_0, v_0).

Near the steady state $S(u_0, v_0)$ in the (u, v) phase plane the null clines $f(u, v) = 0$ and $g(u, v) = 0$ locally can intersect in different ways, for example, as illustrated in Figure 7.2. Note that Figure 7.2(b) is effectively equivalent to Figure 7.2(a): it is simply Figure 7.2(a) rotated. Figure 7.2(c) is qualitatively different from the others.

Let us assume that the kinetics $f(u, v)$ and $g(u, v)$ are such that (7.10) has a confined set in the positive quadrant. Then, by the Poincaré–Bendixson theorem, limit cycle solutions exist if (u_0, v_0) is an unstable spiral or node, but not if it is a saddle point

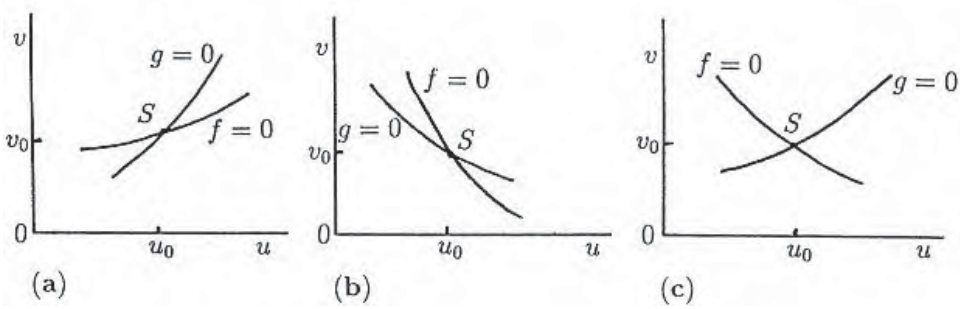

Figure 7.2. Local behaviour of the reaction null clines $f = 0$, $g = 0$ at a steady state $S(u_0, v_0)$.

(see Appendix A). For an unstable node or spiral to occur, we require

$$\mathrm{tr}A > 0, \quad |A| > 0, \quad (\mathrm{tr}A)^2 \begin{cases} > \\ < \end{cases} 4|A| \quad \Rightarrow \quad \text{unstable} \begin{cases} \text{node} \\ \text{spiral} \end{cases}. \tag{7.15}$$

Consider now Figure 7.2(a). At the steady state (u_0, v_0) on each of $f = 0$ and $g = 0$ the gradient $dv/du > 0$ with $dv/du]_{g=0} > dv/du]_{f=0}$, so

$$\left.\frac{dv}{du}\right]_{g=0} = -\frac{g_u}{g_v} > \left.\frac{dv}{du}\right]_{f=0} = -\frac{f_u}{f_v} > 0$$
$$\Rightarrow |A| = f_u g_v - f_v g_u > 0,$$

provided f_v and g_v have the same sign. Since $dv/du > 0$ it also means that at S, f_u and f_v have different signs, as do g_u and g_v. Now from (7.13), $\mathrm{tr}A > 0$ requires at least that f_u and g_v are of opposite sign or are both positive. So, the matrix A (the stability matrix or community matrix in interaction population terms) in (7.12) has terms with the following possible signs for the elements,

$$A = \begin{pmatrix} + & - \\ + & - \end{pmatrix} \quad \text{or} \quad \begin{pmatrix} - & + \\ - & + \end{pmatrix} \tag{7.16}$$

with each of which it is possible to have $\mathrm{tr}\, A > 0$. We have already shown that $|A| > 0$. To proceed further we need to know individually the signs of f_u, f_v, g_u and g_v at the steady state. With Figure 7.2(a) there are 4 possibilities as illustrated in Figure 7.3. These imply that the elements in the matrix A in (7.12) have the following signs,

$$A = \underset{\text{(a)}}{\begin{pmatrix} - & + \\ + & - \end{pmatrix}} \text{ or } \underset{\text{(b)}}{\begin{pmatrix} - & + \\ - & + \end{pmatrix}} \text{ or } \underset{\text{(c)}}{\begin{pmatrix} + & - \\ + & - \end{pmatrix}} \text{ or } \underset{\text{(d)}}{\begin{pmatrix} + & - \\ - & + \end{pmatrix}}. \tag{7.17}$$

For example, to get the sign of f_u at S in Figure 7.3(a) we simply note that as we move along a line parallel to the u-axis through S, f decreases since $f > 0$ on the lower u-side and $f < 0$ on the higher u-side. If we now compare these forms with those in (7.16) we see that the only possible forms in (7.17) are (b) and (c). With (d), $|A| < 0$

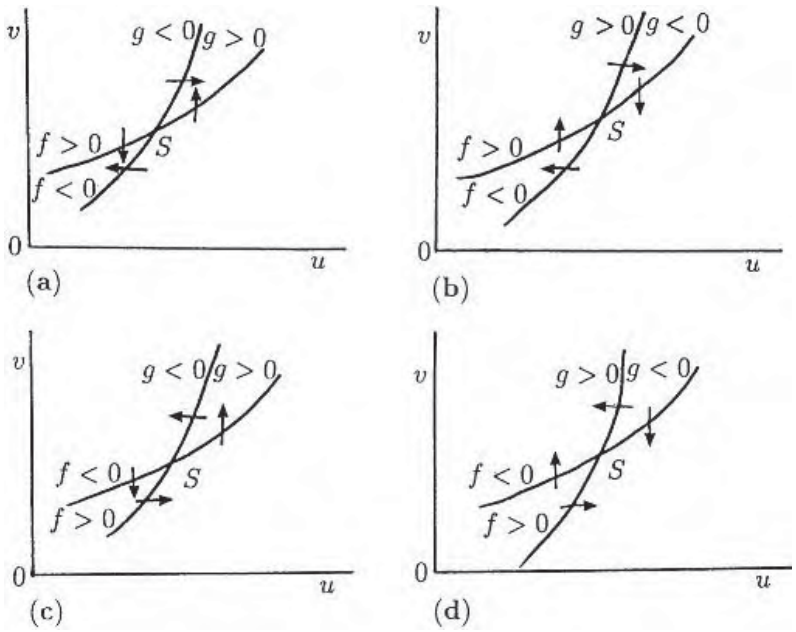

Figure 7.3. The various possible signs of the kinetics functions $f(u, v)$ and $g(u, v)$ on either side of their null clines for the case illustrated in Figure 7.2(a). The arrows indicate, qualitatively, directions of typical trajectories in the neighbourhood of the steady state S.

which makes S a saddle point (which is unstable, of course) and so there can be no limit cycle solution enclosing S (see Appendix A).

For any given kinetics functions it is easy to determine from the null clines the qualitative behaviour in the neighbourhood of a steady state, and hence the signs in the matrix A in (7.12). If the null clines look locally like those in Figures 7.2(b) and (c) similar results can easily be obtained for the allowable type of kinetics which can admit periodic solutions for (7.10).

Let us now consider two typical examples which illustrate the qualitative approach we have just described. Let us suppose a parameter λ of the kinetics is such that the null clines for (7.10) look like those in Figure 7.4 for different ranges of the parameter λ. (This is in fact the null cline situation for the real biological oscillator, Thomas 1975, briefly discussed in Chapter 6, Section 6.7.) To be specific we choose specific signs for f and g on either side of the null clines as indicated (these are in accord with the practical Thomas 1975 kinetics situation). Note that there is a confined set on the boundary of which the vector $(du/dt, dv/dt)$ points into the set: one such set is specifically indicated by $ABCDA$ in Figure 7.4(a).

Let us now consider each case in Figure 7.4 in turn. Figure 7.4(a) is equivalent to that in Figure 7.2(c). Here, in the neighbourhood of S,

$$\left.\frac{dv}{du}\right]_{f=0} = -\frac{f_u}{f_v} < 0, \quad f_u < 0, \quad f_v < 0,$$

$$\left.\frac{dv}{du}\right]_{g=0} = -\frac{g_u}{g_v} > 0, \quad g_u > 0, \quad g_v < 0.$$

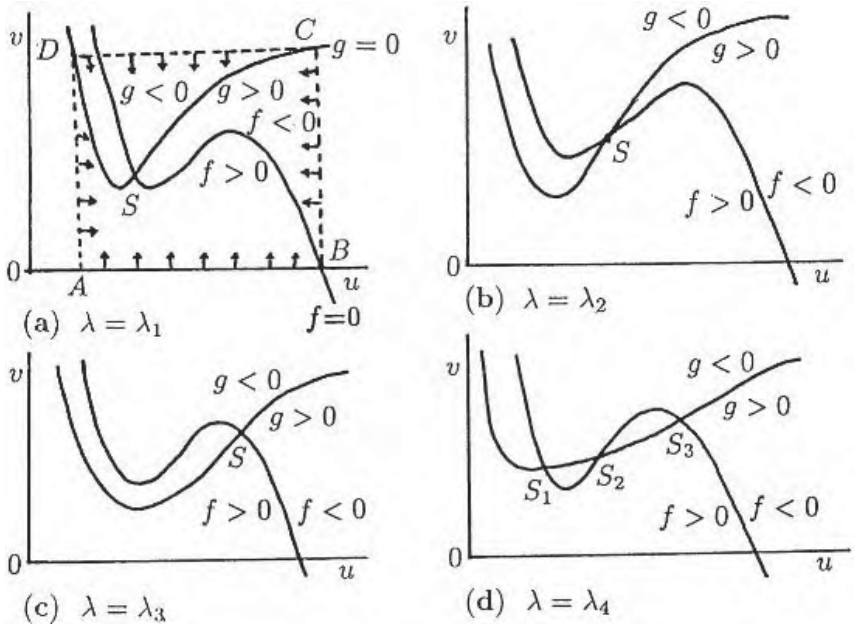

Figure 7.4. Qualitative form of the null clines for a specimen kinetics in (7.10) as a parameter λ varies: $\lambda_1 \neq \lambda_2 \neq \lambda_3 \neq \lambda_4$. With the signs of f and g as indicated, there is a confined set for (7.10): it is, for example, the rectangular box $ABCDA$ as indicated in (**a**).

So, the stability matrix A in (7.12) has the signs

$$A = \begin{pmatrix} - & - \\ + & - \end{pmatrix} \quad \Rightarrow \quad \mathrm{tr}A < 0, \quad |A| > 0$$

which does not correspond to any of the forms in (7.16); from (7.13), $\mathrm{Re}\,\lambda < 0$ and so the steady state in Figure 7.4(a) is always stable and periodic solutions are not possible for (7.10) in this situation. This case, however, is exactly the same as that in Figure 7.4(c) and so the same conclusion also holds for it. By a similar analysis we get for Figure 7.4(b)

$$A = \begin{pmatrix} + & - \\ + & - \end{pmatrix}$$

which is the same as (c) in (7.17), and is one of the possible forms for (7.10) to admit periodic solutions.

If we now consider the multi-steady state situation in Figure 7.4(d), we have already dealt with S_1 and S_3, which are the same as in Figures 7.4(a) and (c)—they are always *linearly* stable. For the steady state S_2 we have

$$\begin{aligned} & f_u > 0, \quad f_v < 0, \quad g_u > 0, \quad g_v < 0 \\ & 0 < \left.\frac{dv}{du}\right]_{g=0} < \left.\frac{dv}{du}\right]_{f=0} \quad \Rightarrow \quad 0 < -\frac{g_u}{g_v} < -\frac{f_u}{f_v} \\ & \Rightarrow |A| = f_u g_v - f_v g_u < 0, \end{aligned}$$

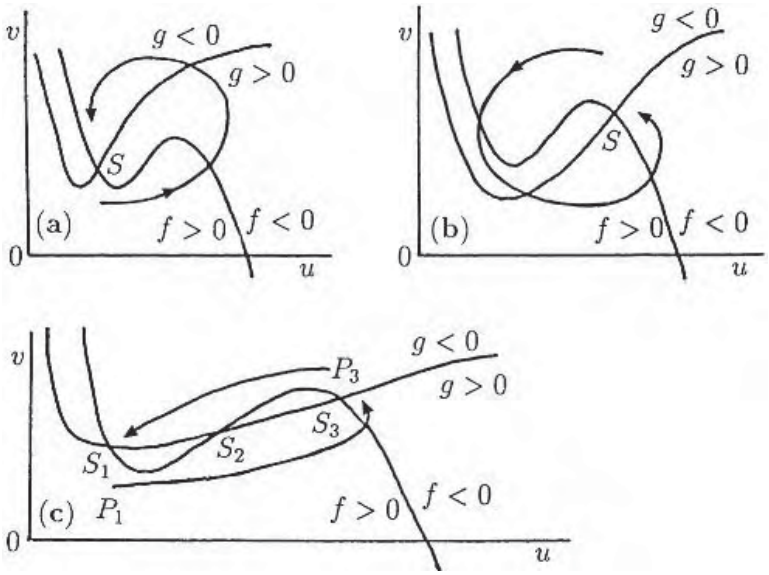

Figure 7.5. Threshold phenomena for various kinetics for (7.10). In (**c**) a suitable perturbation from one linearly stable steady state can effect a permanent change to the other stable steady state.

which, from (7.15), shows that the steady state is a saddle point, and although it means S_2 is unstable, it is the type of singularity which does not admit periodic solutions for (7.10) according to the Poincaré–Bendixson theorem (Appendix A).

This last case, Figure 7.4(d), is of considerable general importance. Recall the threshold phenomenon described in the last chapter in Section 6.7. There we saw that in a situation similar to that in Figures 7.4(a) and (c) that, although the steady state is linearly stable, if a perturbation is sufficiently large the values of u and v can undergo large perturbations before returning to the steady state (refer to Figure 6.10). This phenomenon is illustrated in Figures 7.5(a) and (b).

Now consider Figure 7.4(d). S_1 and S_3 are respectively equivalent to the S in Figures 7.5(a) and (b). We now see, in Figure 7.5(c), that if we perturb (u, v) from say, S_1 to P_1, the solution trajectory will be qualitatively as shown. Now, instead of returning to S_1 the solution moves to S_3, the second stable steady state. In this way a *switch* has been effected from S_1 to S_3. In a similar way a switch can be effected from S_3 to S_1 by, for example, a perturbation from the steady state S_3 to P_3. It is possible that a parameter in the kinetics function g, say, can be varied in such a way that the null cline is translated vertically as the parameter is, for example, increased. In this case it is possible for the system to exhibit *hysteresis* such as we discussed in detail in Chapter 1, Section 1.2 and Chapter 6, Section 6.7. If the reaction kinetics give rise to mushrooms and isolas, even more baroque dynamic, threshold and limit cycle behaviour is possible. Biological switches, not only those exhibiting hysteresis and more exotic behaviour, are of considerable importance in biology. We discuss one important example below in Section 7.5. We also see a specific example of its practical importance in the wave phenomenon observed in certain eggs after fertilization, a process and mechanism for which is discussed in detail in Chapter 13, Section 13.6 below and Chapter 6, Volume II, Section 6.8.

It is clear from the above that the qualitative behaviour of the solutions can often be deduced from a gross geometric study of the null clines and the global phase plane

behaviour of trajectories. We can carry this approach much further, as has been done, for example by Rinzel (1986), to predict even more complex solution behaviour of such differential equation systems. Here I only want to give a flavour of what can be found.

Let us suppose we have a general system governed by

$$\frac{d\mathbf{u}}{dt} = \mathbf{f}(\mathbf{u}, \alpha), \quad \frac{d\alpha}{dt} = \varepsilon g(\mathbf{u}, \alpha), \tag{7.18}$$

where $0 < \varepsilon \ll 1$, $\mathbf{u}$ is a vector of concentrations and α is a parameter, which is itself governed by an equation, but which changes only slowly. The *fast* subsystem of (7.18) is the $O(1)$ system, as $\varepsilon \to 0$, in which α is simply a constant parameter, since $d\alpha/dt \approx 0$. The *slow* dynamics governs the change in α with time. We analyse some specific systems like this in the following chapter, when we discuss relaxation oscillators.

Suppose a uniform steady state $\mathbf{u}_0$ depends on α as indicated schematically in Figure 7.6(a). That is, there is a region $\alpha_1 < \alpha < \alpha_2$ where three possible steady states $\mathbf{u}_0$ exist; recall also the discussion in Section 6.7 in the last chapter. To be more specific let us suppose that α varies periodically in such a way that in each cycle it sweeps back and forth through the window which gives three solutions for $\mathbf{u}_0$, the one on the dashed line in Figure 7.6(a) being unstable as to be expected. At the start suppose $\alpha = \alpha_1$ and $\mathbf{u}_0$ is at A in Figure 7.6(a). Now as α increases, $\mathbf{u}_0$ slowly varies until α passes through α_2. At α_2, $\mathbf{u}_0$ jumps discontinuously from B to C, after which it again varies slowly with α. On the return α-trip, $\mathbf{u}_0$ remains on the lower branch of the S-curve until it reaches D, where it jumps up to A again. The limit cycle behaviour of this system is illustrated schematically in Figure 7.6(b). The rapidly varying region is where $\mathbf{u}$ drops from B to C and increases from D to A. This is a typical *relaxation oscillator* behaviour; see Chapter 8, Section 8.4 below.

The fast dynamics subsystem in (7.18) may, of course, have as its steady state a periodic solution, say, $\mathbf{u}_{\text{per}}$. Now the parameter α affects an oscillatory solution. A relevant bifurcation diagram is then one which shows, for example, a transition from one oscillation to another. Figure 7.7(a) illustrates such a possibility. The branch AB represents, say, a small amplitude stable limit cycle oscillation around $\mathbf{u}_0$ for a given α.

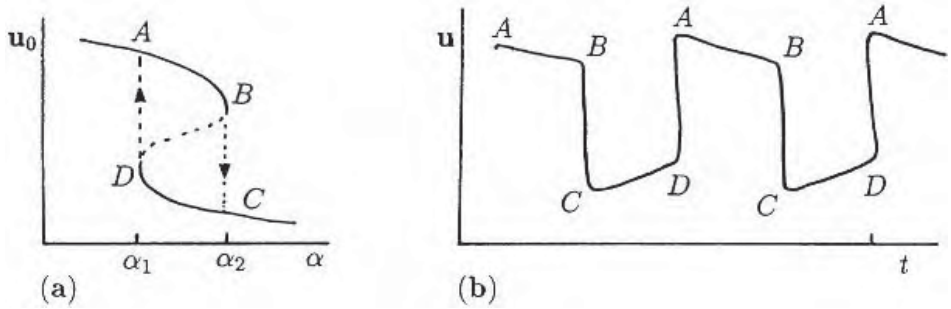

Figure 7.6. (**a**) Schematic steady state $\mathbf{u}_0$ dependence on the parameter α: steady states on the dashed line are unstable. (**b**) Typical limit cycle behavior of $\mathbf{u}$ if α slowly varies in a periodic way. The oscillation is described as a *relaxation oscillator*: that is, there are slowly varying sections of the solution interspersed with rapidly varying regions.

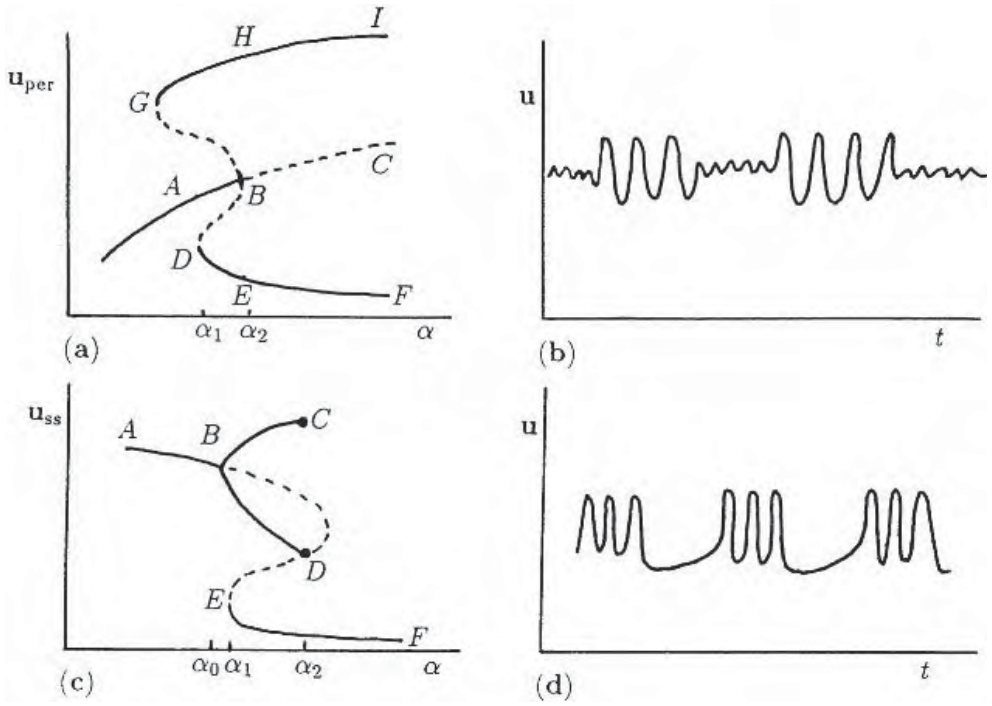

Figure 7.7. (**a**) Schematic bifurcation for periodic solutions of the fast dynamics subsystem of (7.18) as α varies periodically. The dashed lines are unstable branches. (**b**) Typical periodic behaviour as α slowly varies in a periodic way back and forth through the (α_1, α_2) window, for the bifurcation picture in (**a**). (**c**) Another example of a periodic solution bifurcation diagram for the subsystem of (7.18) as α varies. (**d**) Qualitative periodic solution behaviour as α varies periodically through α_1 and α_2 in (**c**). These are examples of 'periodic bursting.'

Solutions on the branch BC are unstable. Now as α increases there is a slow variation in the solution until it passes through α_2 at B, after which the periodic solution undergoes a bifurcation to a larger amplitude oscillation with bounds for $\mathbf{u}$ on the curves EF and HI. The transition from one solution type to another is fast, as in the relaxation oscillator situation in Figure 7.6. Now let α decrease. The bifurcation to the AB branch now occurs at D, where $\alpha = \alpha_1$. So, as α varies periodically such that it includes a window with $\alpha < \alpha_1$ and $\alpha > \alpha_2$, the solution behaviour will be qualitatively like that shown in Figure 7.7(b).

Figure 7.7(c) shows another possible example. The line AB represents a nonoscillatory solution which bifurcates for $\alpha = \alpha_0$ to a periodic solution at B. These branches terminate at D and C, where $\alpha = \alpha_2$. The branch EF is again a uniform stable steady state. Suppose we now consider α to vary periodically between $\alpha > \alpha_2$ and $\alpha_0 < \alpha < \alpha_1$. To be specific, let us start at F in Figure 7.7(c). As α decreases we move along the branch FE; that is, the uniform steady state $\mathbf{u}_{ss}$ varies slowly. At E, where $\alpha = \alpha_1$, the uniform steady state bifurcates to a periodic solution on the branches BD and BC. Now as α increases the periodic solution remains on these branches until α reaches α_2 again, after which the solution jumps down again to the homogeneous steady state branch EF. A typical time behaviour for the solution is illustrated in Figure 7.7(d). Both this behaviour and that in Figure 7.7(b) are described as 'periodic bursting.' Keener and Sneyd (1998) devote a chapter to this phenomenon and describe some specific models of biological examples where it occurs.

The complexity of solution behaviour of such systems (7.18) can be spectacular. The specific behaviour just described in Figures 7.6 and 7.7 has been found in models for real biological systems; an example of the former is in the following chapter, while qualitatively similar curves to those in Figure 7.7 have been found by Rinzel (1985). The system studied by Rinzel (1985) is specifically related to the model described below in Section 7.5 on neural periodic behaviour. The model system given by (6.125) in Section 6.7 in the last chapter, and the iodate–arsenous model reaction scheme (6.132) and (6.133), exhibit comparable solution behaviour but with the potential for even more complex dynamic phenomena. Othmer and Schaap (1999) discuss the kinetics (firmly based on the biology) associated with cyclic-AMP emission by cells of the slime mould *Dictyostelium discoideum*; see also the article by Dallon and Othmer (1997) who put forward a discrete cell model for its adaptive signalling. This slime mould exhibits some remarkable complex dynamics. Decroly and Goldbeter (1987) considered a model 3-variable system associated with cyclic-AMP emission by the cells of *Dictyostelium discoideum* as a vehicle to demonstrate the transition from simple to complex oscillatory behaviour. As well as obtaining increasingly complex patterns of bursting they showed period doubling leading to chaos; see also Goldbeter (1996).

Figure 7.7 shows some of the complex effects which appear when oscillators interact or when reaction schemes have fast and slow subschemes. This is mathematically a very interesting and challenging field and one of continuing research. We consider in some detail some important aspects of oscillator interaction in Chapter 9. In Chapter 12 we discuss another important and quite different aspect of interacting oscillations.

Canards

A canard is the word associated with oscillatory systems which undergo sudden major changes in the amplitude and period of the oscillatory solution as some parameter passes through a narrow range of values. Canards were first discussed in association with the van der Pol equation by Benoit et al. (1981) and have been studied since in a variety of applications. Canard systems give rise to interesting and sometimes baroque dynamical behaviour. The discovery of canards in relatively simple chemical reaction systems stems from the second half of the 1980's; one is the two-variable Oregonator (Brøns and Bar-Eli 1991), a system we discuss in some detail in Chapter 8.

Canards were found by Gáspár and Showalter (1990) in the oscillatory iodate–sulphite–ferrocyanide reaction, known as the EOB reaction which was discovered by Edblom and Epstein (1986). The analysis of these sytems can be quite complicated and analytically interesting since, among other things, they usually involve the interplay of fast and slow dynamics and hence singular perturbation theory is generally appropriate. The EOB reaction can be described by a ten-variable empirical-rate-law model system which like the Belousov–Zhabotinsky reaction (see Chapter 8) can be reduced (Gáspár and Showalter 1990) in this case to a four-variable system which retains the essential experimental features of the full system. This four-variable system is given by

$$A + Y \underset{k_{-1}}{\overset{k_1}{\rightleftharpoons}} X, \quad X \overset{k_2}{\to} Y, \quad 2Y \overset{k_3}{\to} Z, \quad Z + X \overset{k_4}{\to} 3Y, \quad Z \overset{k_5}{\to},$$

where $A = SO_3^{2-}$, $X = HSO_3^-$, $Y = H^+$ and $Z = I_2$. Gáspár and Showalter (1990) used a singular perturbation approach which eliminated the A and Z variables and obtained the minimal set of equations

$$\frac{dX}{dt} = k_1 A_s Y - (k_{-1} + k_2 + k_4 Z_s + k_0)X,$$
$$\frac{dY}{dt} = -k_1 A_s Y + (k_{-1} + k_2 + 3k_4 Z_s)X - 2k_3 Y^2 + k_0(Y_0 - Y),$$

where A_s and Z_s are functions of X and Y given by

$$A_s = \frac{k_{-1}X + k_0 A_0}{k_1 Y + k_0}, \quad Z_s = \frac{k_3 Y^2}{k_1 X + k_5 + k_0}$$

and k_0, A_0 and Y_0 are constants associated with the experimental parameters. Peng et al. (1991) analyse this system and other practical model chemical systems which display canards.

7.4 Simple Two-Species Oscillators: Parameter Domain Determination for Oscillations

If we restrict our reaction system to only two species it was shown by Hanusse (1972) that limit cycle solutions can only exist if there are trimolecular reactions. These would be biochemically unrealistic if they were the only reactions involved, but as we have shown in Chapter 6 such two-reactant models can arise naturally from a higher-order system if typical enzyme reactions, for example, are part of the mechanism being considered. So, it is reasonable to consider trimolecular two-species models and not just for algebraic and mathematical convenience in demonstrating principles and techniques. Schnackenberg (1979) considered the class of two-species 'simplest,' but chemically plausible, trimolecular reactions which will admit periodic solutions. The simplest such reaction mechanism is

$$X \underset{k_{-1}}{\overset{k_1}{\rightleftharpoons}} A, \quad B \overset{k_2}{\to} Y, \quad 2X + Y \overset{k_3}{\to} 3X, \tag{7.19}$$

which, using the Law of Mass Action, results in the nondimensional equations for u and v, the dimensionless concentrations of X and Y, given by

$$\frac{du}{dt} = a - u + u^2 v = f(u, v), \quad \frac{dv}{dt} = b - u^2 v = g(u, v), \tag{7.20}$$

where a and b are positive constants. Typical null clines are illustrated in Figure 7.8. In the vicinity of the steady state S these are equivalent to the situation in Figure 7.2(b). With (7.20) it is easy to construct a confined set on the boundary of which the vector $(du/dt, dv/dt)$ points inwards or along it; the quadrilateral in Figure 7.8 is one example. Hence, because of the Poincaré–Bendixson theorem, the existence of a peri-

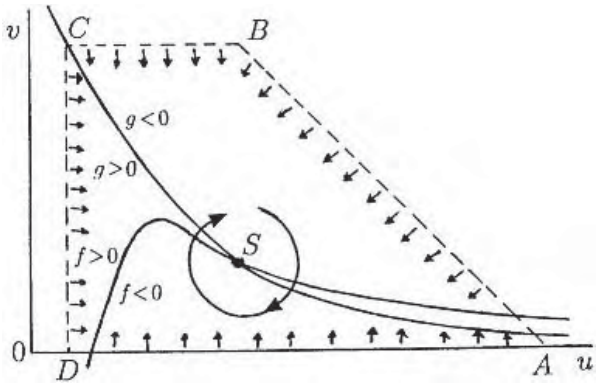

Figure 7.8. Typical null clines $f = 0$ and $g = 0$ for the 'simplest' oscillator (7.20) for $a > 0$ and $b > 0$. The quadrilateral *ABCDA* is a boundary of a confined set enclosing the steady state *S*.

odic solution is assured if, for (7.20), the stability matrix A for the steady state satisfies (7.15).

Determination of Parameter Space for Oscillations

For any model involving parameters it is always useful to know the ranges of parameter values where oscillatory solutions are possible and where they are not. For all but the simplest kinetics this has to be done numerically, but the principles involved are the same for them all. Here we carry out the detailed analysis for the simple model reaction (7.20) to illustrate the general principles: the model involves only two parameters a and b and we can calculate the (a, b) parameter space analytically. The requisite space is the range of the parameters a and b which make the steady state an unstable node or spiral: that is, the parameter range where, from (7.15), $\mathrm{tr}A > 0$ and $|A| > 0$. Later we shall develop a more powerful and general parametric method which can be applied to less simple kinetics.

The steady state (u_0, v_0) for (7.20) is given by

$$\begin{aligned} &f(u_0, v_0) = a - u_0 + u_0^2 v_0 = 0, \quad g(u_0, v_0) = b - u_0^2 v_0 = 0, \\ &\Rightarrow u_0 = b + a, \quad v_0 = \frac{b}{(a+b)^2}, \quad \text{with} \quad b > 0,\ a + b > 0. \end{aligned} \tag{7.21}$$

Substituting these into the stability matrix A in (7.12), we get

$$\begin{aligned} &\mathrm{tr}A = f_u + g_v = (-1 + 2u_0 v_0) + (-u_0^2) = \frac{b-a}{a+b} - (a+b)^2, \\ &|A| = f_u g_v - f_v g_u = (a+b)^2 > 0 \quad \text{for all} \quad a, b. \end{aligned} \tag{7.22}$$

The domain in (a, b) space where (u_0, v_0) is an unstable node or spiral is, from (7.15), where $\mathrm{tr}A > 0$ and so the domain boundary is

$$\mathrm{tr}A = 0 \quad \Rightarrow \quad b - a = (a+b)^3. \tag{7.23}$$

Even with this very simple model, determination of the boundary involves the solution of a cubic, not admittedly a major problem, but a slightly tedious one. Care has

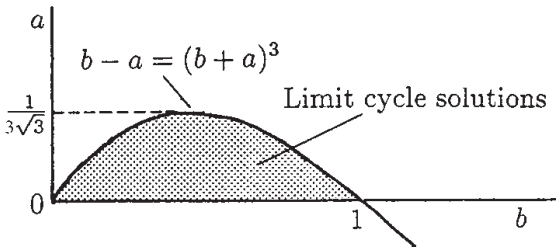

Figure 7.9. Parameter space where limit cycle periodic solutions of (7.20) exist for $a > 0$ and $b > 0$. The boundary curve is given by (7.23), although it was in fact calculated using the more easily applied parametric form (7.27).

to be taken since the solution, say, of b in terms of a, involves three branches. Figure 7.9 gives the parameter domain where oscillations are possible for $b > 0$. There is another more powerful way (Murray 1982) of determining the boundary, namely, parametrically, which is much easier and which also avoids the multiple branch problem. Furthermore, it is a method which has wider applicability, can be used with more complicated systems and provides the numerical procedure for the determination of the parameter domain for systems where it is not feasible to do it analytically. We again use the simple model system (7.20) to illustrate the method; see the exercises for other examples.

Let us consider the steady state u_0 as a parameter and determine b and a in terms of u_0. From (7.21),

$$v_0 = \frac{u_0 - a}{u_0^2}, \quad b = u_0^2 v_0 = u_0 - a, \tag{7.24}$$

and

$$A = \begin{pmatrix} f_u & f_v \\ g_u & g_v \end{pmatrix} = \begin{pmatrix} -1 + 2u_0 v_0 & u_0^2 \\ -2u_0 v_0 & -u_0^2 \end{pmatrix} = \begin{pmatrix} 1 - \dfrac{2a}{u_0} & u_0^2 \\ -2 + \dfrac{2a}{u_0} & -u_0^2 \end{pmatrix}.$$

Since $|A| = u_0^2 > 0$ the required necessary condition for oscillations from (7.15) is $\mathrm{tr}A > 0$; that is,

$$f_u + g_v > 0 \quad \Rightarrow \quad 1 - \frac{2a}{u_0} - u_0^2 > 0 \quad \Rightarrow \quad a < \frac{u_0(1 - u_0^2)}{2}. \tag{7.25}$$

We also have from (7.24)

$$b = u_0 - a > \frac{u_0(1 + u_0^2)}{2}. \tag{7.26}$$

The last two inequalities define, parametrically in u_0, the boundary curve where $\mathrm{tr}A = 0$. Since the parameter u_0 is the steady state, the only parameter range of interest is $u_0 \geq 0$. Thus, one of the boundary curves in (a, b) space, which defines the domain where the necessary condition for oscillations is satisfied (in this example it is only $\mathrm{tr}A > 0$), is defined by

$$a = \frac{u_0(1-u_0^2)}{2}, \quad b = \frac{u_0(1+u_0^2)}{2}, \quad \text{for all} \quad u_0 > 0. \tag{7.27}$$

Sufficient conditions for an oscillatory solution are given by (7.15) together with the existence of a confined set. Since a confined set has been obtained for this mechanism (see Figure 7.8) the conditions (7.25) and (7.26) are sufficient. Figure 7.9 was calculated using (7.27) and shows the space given by (7.23). The mechanism (7.20) will exhibit a limit cycle oscillation for any parameter values which lie in the shaded region; for all other values in the positive quadrant the steady state is stable.

This pedagogically very useful model (7.20) is a particularly simple one for which to determine the parameter space for periodic solutions. This is because the requirement $|A| > 0$ was automatically satisfied for all values of the parameter and the necessary and sufficient condition for existence boiled down to finding the domain where $\mathrm{tr}A$ was positive. Generally, once a confined set has been found (which in itself can often put constraints on the parameters), the parameter space for periodic solutions is determined by the *two* boundary curves in parameter space defined by $\mathrm{tr}A = 0$, $|A| = 0$.

Although we envisage the biochemical mechanism (7.20) to have $a > 0$ the mathematical problem need not have such a restriction as long as u_0 and v_0 are nonnegative.

To show how the parametric procedure works in general, let us allow a to be positive or negative. Now the necessary and sufficient conditions are satisfied if $\mathrm{tr}A > 0$, namely, (7.25) with (7.26), and $|A| > 0$. Since $|A| = u_0^2 > 0$, the condition $|A| > 0$ is automatically satisfied. With the requirement $u_0 \geq 0$ this gives the curve in (a, b) space as

$$b + a > 0 \quad \Rightarrow \quad a > -u_0, \quad b > u_0, \tag{7.28}$$

as a particularly simple parametric representation. Thus the two sets of inequalities are bounded in parameter space by the curves

$$\left.\begin{array}{ll} a = \dfrac{u_0(1-u_0^2)}{2}, & b = \dfrac{u_0(1+u_0^2)}{2}, \\ a = -u_0 & b = u_0 \end{array}\right\} \quad \text{for all} \quad u_0 \geq 0. \tag{7.29}$$

Figure 7.10 gives the general parameter space defined by (7.29). The inequality (7.28)

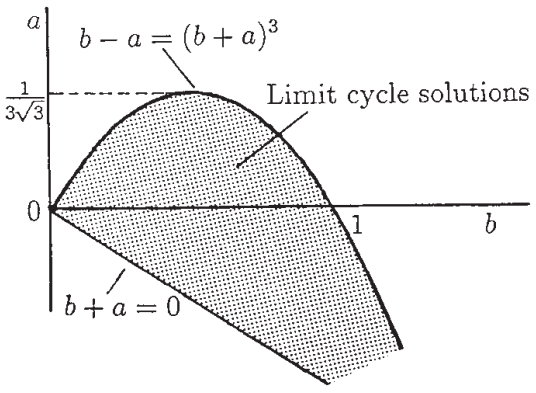

Figure 7.10. Parameter space in which solutions (u, v) of (7.20) are periodic limit cycles. Note that $a < 0$ is possible, although it is not of biochemical interest.

is satisfied by values (a, b) which lie above the straight line given by (7.29) while the inequality (7.26) is satisfied for values lying below the curve given by (7.29). Together they define a closed domain.

$\lambda - \omega$ Systems

These are particularly simple systems of equations which have exact limit cycle solutions, and which have been widely used in prototype studies of reaction diffusion systems. The equations can be written in the form

$$\begin{aligned} &\frac{du}{dt} = \lambda(r)u - \omega(r)v, \quad \frac{dv}{dt} = \omega(r)u + \lambda(r)v, \\ &r = (u^2 + v^2)^{1/2}, \end{aligned} \tag{7.30}$$

where λ is a positive function of r for $0 \leq r \leq r_0$ and negative for $r > r_0$, and so $\lambda(r_0) = 0$, and $\omega(r)$ is a positive function of r. It does not seem possible to derive such equations from any sequence of reasonable biochemical reactions. However, their advantage primarily lies in the fact that explicit analytic results can be derived when they are used as the kinetics in the study of wave phenomena in reaction diffusion models. Such analytical solutions can often provide indications of what to look for in more realistic systems. So although their use is in an area discussed later, it is appropriate to introduce them here simply as examples of nontrivial mathematical oscillators.

If we express the variables (u, v) in the complex form $c = u + iv$, equations (7.30) become the complex equation

$$\frac{dc}{dt} = [\lambda(|c|) + i\omega(|c|)]c, \quad c = u + iv. \tag{7.31}$$

From this, or by multiplying the first of (7.30) by u and adding it to v times the second, we see that a limit cycle solution is a circle in the (u, v) plane or complex c-plane since

$$\frac{d|c|}{dt} = \lambda(|c|)|c| \quad \Rightarrow \quad |c| = r_0, \tag{7.32}$$

because $\lambda(|c|)$ is positive if $0 \leq |c| < r_0$ and negative if $|c| > r_0$.

An alternative way to write (7.31) in the complex plane is to set

$$c = re^{i\theta} \quad \Rightarrow \quad \frac{dr}{dt} = r\lambda(r), \quad \frac{d\theta}{dt} = \omega(r) \tag{7.33}$$

for which the limit cycle solution is

$$r = r_0, \quad \theta(t) = \omega(r_0)t + \theta_0, \tag{7.34}$$

where θ_0 is a constant.

7.5 Hodgkin–Huxley Theory of Nerve Membranes: FitzHugh–Nagumo Model

Neural communication is clearly a very important field. We make no attempt here to give other than a basic introduction to it and discuss one of the key mathematical models which has been studied extensively. Rinzel (1981) gives a short review of models in neurobiology; see also Keener and Sneyd (1998).

Electric signalling or firing by individual nerve cells or neurons is particularly common. The seminal and now classical work by Hodgkin and Huxley (1952) on this aspect of nerve membranes was on the nerve axon of the giant squid. (They were awarded a Nobel prize for their work.) Basically the axon is a long cylindrical tube which extends from each neuron and electrical signals propagate along its outer membrane, about 50 to 70 Ångströms thick. The electrical pulses arise because the membrane is preferentially permeable to various chemical ions with the permeabilities affected by the currents and potentials present. The key elements in the system are potassium (K^+) ions and sodium (Na^+) ions. In the rest state there is a transmembrane potential difference of about -70 millivolts (mV) due to the higher concentration of K^+ ions within the axon as compared with the surrounding medium. The deviation in the potential across the membrane, measured from the rest state, is a primary observable in experiments. The membrane permeability properties change when subjected to a stimulating electrical current I: they also depend on the potential. Such a current can be generated, for example, by a local depolarisation relative to the rest state.

In this section we are concerned with the *space-clamped* dynamics of the system; that is, we consider the spatially homogeneous dynamics of the membrane. With a real axon the space-clamped state can be obtained experimentally by having a wire down the middle of the axon maintained at a fixed potential difference to the outside. Later, in Chapter 1, Volume II, we shall discuss the important spatial propagation of action potential impulses along the nerve axon; we shall refer back to the model we discuss here. We derive here the Hodgkin–Huxley (1952) model and the reduced analytically tractable FitzHugh–Nagumo mathematical model (FitzHugh 1961, Nagumo et al. 1962) which captures the key phenomena. The analysis of the various mathematical models has indicated phenomena which have motivated considerable experimental work. The theory of neuron firing and propagation of nerve action potentials is one of the major successes of real mathematical biology.

Basic Mathematical Model

Let us take the positive direction for the membrane current, denoted by I, to be outwards from the axon. The current $I(t)$ is made up of the current due to the individual ions which pass through the membrane and the contribution from the time variation in the transmembrane potential, that is, the membrane capacitance contribution. Thus we have

$$I(t) = C\frac{dv}{dt} + I_i, \tag{7.35}$$

where C is the capacitance and I_i is the current contribution from the ion movement across the membrane. Based on experimental observation Hodgkin and Huxley (1952) took

$$\begin{aligned} I_i &= I_{Na} + I_K + I_L, \\ &= g_{Na} m^3 h(V - V_{Na}) + g_K n^4 (V - V_K) + g_L (V - V_L), \end{aligned} \tag{7.36}$$

where V is the potential and I_{Na}, I_K and I_L are respectively the sodium, potassium and 'leakage' currents; I_L is the contribution from all the other ions which contribute to the current. The g's are constant conductances with, for example, $g_{Na} m^3 h$ the sodium conductance, and V_{Na}, V_K and V_L are constant equilibrium potentials. The m, n and h are variables, bounded by 0 and 1, which are determined by the differential equations

$$\begin{aligned} \frac{dm}{dt} &= \alpha_m(V)(1 - m) - \beta_m(V)m, \\ \frac{dn}{dt} &= \alpha_n(V)(1 - n) - \beta_n(V)n, \\ \frac{dh}{dt} &= \alpha_h(V)(1 - h) - \beta_h(V)h, \end{aligned} \tag{7.37}$$

where the α and β are given functions of V (again empirically determined by fitting the results to the data); see, for example, Keener and Sneyd (1998). α_n and α_m are qualitatively like $(1 + \tanh V)/2$ while $\alpha_h(V)$ is qualitatively like $(1 - \tanh V)/2$, which is a 'turn-off' switch if V is moderately large. Hodgkin and Huxley (1952) fitted the data with exponential forms.

If an applied current $I_a(t)$ is imposed the governing equation using (7.35) becomes

$$C\frac{dV}{dt} = -g_{Na} m^3 h(V - V_{Na}) - g_K n^4 (V - V_K) - g_L (V - V_L) + I_a. \tag{7.38}$$

The system (7.38) with (7.37) constitute the 4-variable model which was solved numerically by Hodgkin and Huxley (1952).

If $I_a = 0$, the rest state of the model (7.37) and (7.38) is linearly stable but is excitable in the sense discussed in Chapter 6. That is, if the perturbation from the steady state is sufficiently large there is a large excursion of the variables in their phase space before returning to the steady state. If $I_a \neq 0$ there is a range of values where regular repetitive firing occurs; that is, the mechanism displays limit cycle characteristics. Both types of phenomena have been observed experimentally. Because of the complexity of the equation system various simpler mathematical models, which capture the key features of the full system, have been proposed, the best known and particularly useful one of which is the FitzHugh–Nagumo model (FitzHugh 1961, Nagumo et al. 1962), which we now derive.

The timescales for m, n and h in (7.37) are not all of the same order. The timescale for m is much faster than the others, so it is reasonable to assume it is sufficiently fast that it relaxes immediately to its value determined by setting $dm/dt = 0$ in (7.37). If we also set $h = h_0$, a constant, the system still retains many of the features experi-

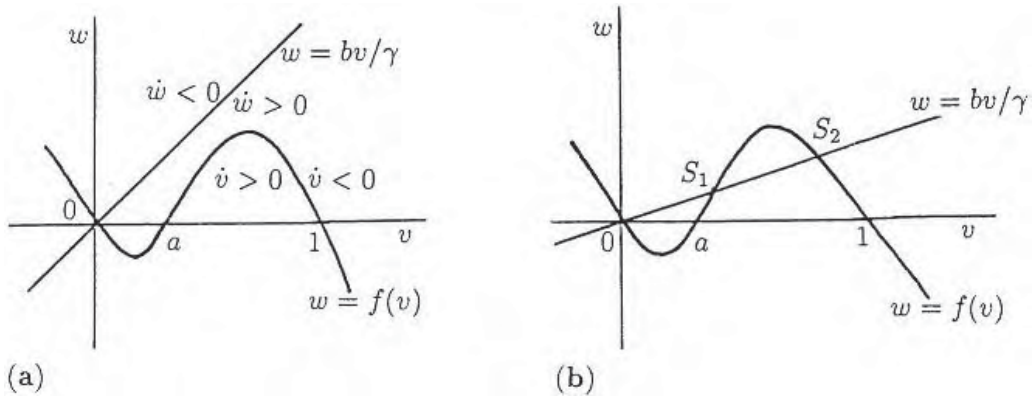

Figure 7.11. Phase plane for the model system (7.39) with $I_a = 0$. As the parameters vary there can be (**a**) one stable, but excitable state or, (**b**) three possible steady states, one unstable, namely, S_1, and two stable, but excitable, namely, (0, 0) and S_2.

mentally observed. The resulting 2-variable model in V and n can then be qualitatively approximated by the dimensionless system

$$\begin{aligned} \frac{dv}{dt} &= f(v) - w + I_a, \quad \frac{dw}{dt} = bv - \gamma w, \\ f(v) &= v(a - v)(v - 1), \end{aligned} \tag{7.39}$$

where $0 < a < 1$ and b and γ are positive constants. Here v is like the membrane potential V, and w plays the role of all three variables m, n and h in (7.37).

With $I_a = 0$, or just a constant, the system (7.39) is simply a 2-variable phase plane system, the null clines for which are illustrated in Figure 7.11. Note how the

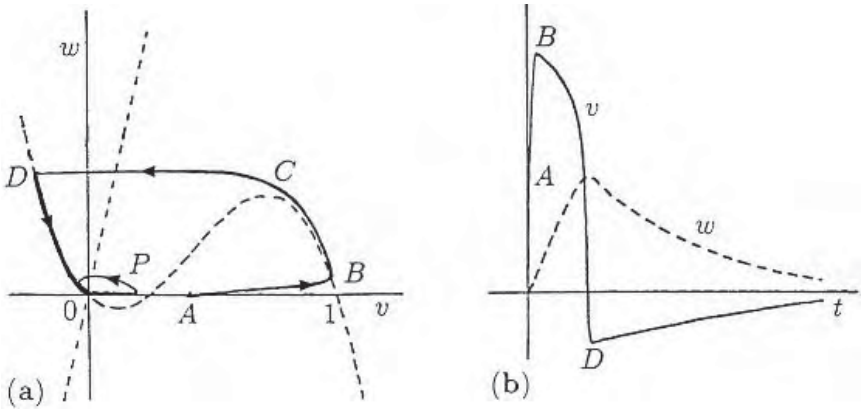

Figure 7.12. (**a**) The phase portrait for (7.39) with $I_a = 0$, $a = 0.25$, $b = \gamma = 2 \times 10^{-3}$ which exhibits the threshold behaviour. With a perturbation from the steady state $v = w = 0$ to a point, P say, where $w = 0$, $v < a$, the trajectory simply returns to the origin with v and w remaining small. A perturbation to A initiates a large excursion along $ABCD$ and then back to (0, 0), effectively along the null cline since b and γ are small. (**b**) The time variation of v and w corresponding to the excitable trajectory $ABCD0$ in (**a**). (Redrawn from Rinzel 1981)

phase portrait varies with different values of the parameters a, b and γ. There can, for example, be 1 or 3 steady states as shown in Figures 7.11(a) and (b) respectively. The situation corresponds to that illustrated in Figure 7.5, except that here it is possible for v to be negative—it is an electric potential. The excitability characteristic, a key feature in the Hodgkin–Huxley system, is now quite evident. That is, a perturbation, for example, from 0 to a point on the v-axis with $v > a$, undergoes a large phase trajectory excursion before returning to 0. Figure 7.12 shows a specific example.

Periodic Neuron Firing

With $I_a = 0$ the possible phase portraits, as illustrated in Figure 7.11, show there can be no periodic solutions (see Section 7.3). Suppose now that there is an applied current I_a. The corresponding null clines for (7.39) are illustrated in Figures 7.13(a) to (c) for several $I_a > 0$. The effect on the null clines is simply to move the v null cline, with $I_a = 0$, up the w-axis. With parameter values such that the null clines are as in Figure 7.13(a) we can see that by varying only I_a there is a window of applied currents (I_1, I_2) where the steady state can be unstable and limit cycle oscillations possible, that is, a null cline situation like that in Figure 7.13(b). The algebra to determine the various parameter ranges for a, b, γ and I_a for each of these various possibilities to hold is straightforward. It is just an exercise in elementary analytical geometry, and is left as an exercise (Exercise 7). With the situation exhibited in Figure 7.13(d) limit cycle solutions are not possible. On the other hand this form can exhibit switch properties.

The FitzHugh–Nagumo model (7.39) is a *model* of the Hodgkin–Huxley *model*. So, a further simplification of the mechanism (7.39) is not unreasonable if it simplifies the analysis or makes the various solution possibilities simpler to see. Of course such a simplification must retain the major elements of the original, so care must be exercised.

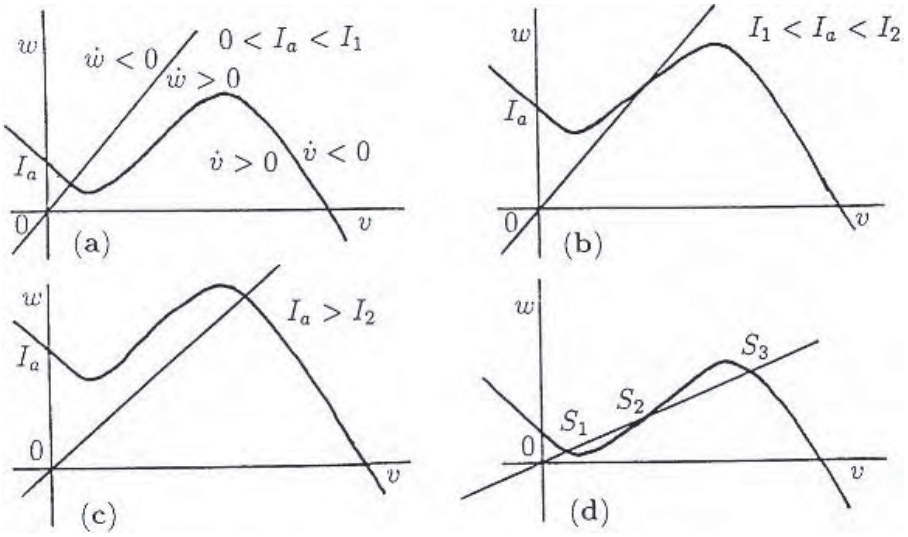

Figure 7.13. Null clines for the FitzHugh–Nagumo model (7.39) with different applied currents I_a. Cases (**a**), where $I_a < I_1$, and (**c**), where $I_a > I_2$, have linearly stable, but excitable, steady states, while in (**b**), where $I_1 < I_a < I_2$, the steady state can be unstable and limit cycle periodic solutions are possible. With the configuration (**d**), the steady states S_1, S_3 are stable with S_2 unstable. Here a perturbation from either S_1 or S_3 can effect a switch to the other.

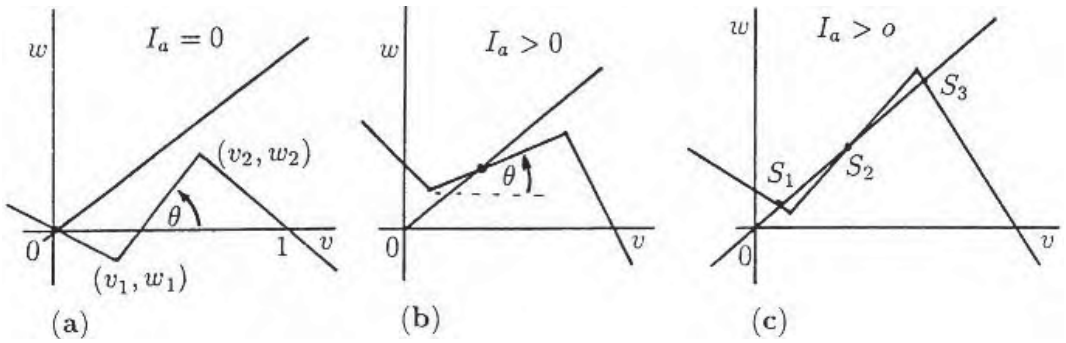

Figure 7.14. (**a**) Phase plane null clines for a piecewise linear approximation to the v null cline in the FitzHugh–Nagumo model (7.30) with $I_a = 0$, where (v_1, w_1) and (v_2, w_2) are given by (7.40). (**b**) The geometric conditions for possible periodic solutions, which require $I_a > 0$, are shown in terms of the angle $\theta = \tan^{-1}[(w_2 - w_1)/(v_2 - v_1)]$. (**c**) Geometric conditions for multiple roots and threshold switch possibilities from one steady state S_1 to S_3 and vice versa.

From Figure 7.11 we can reasonably approximate the v null cline by a piecewise linear approximation as in Figure 7.14, which in Figure 7.14(a) has zeros at $v = 0, a, 1$. The positions of the minimum and maximum, (v_1, w_1) and (v_2, w_2) are obtained from (7.39) as

$$\begin{aligned} v_2, v_1 &= \frac{1}{3}\left[a + 1 \pm \left\{(a+1)^2 - 3a\right\}^{1/2}\right], \\ w_i &= -v_i(a - v_i)(1 - v_i) + I_a, \quad i = 1, 2. \end{aligned} \tag{7.40}$$

The line from (v_1, w_1) to (v_2, w_2) passes through $v = a$ if $a = 1/2$. The acute angle θ the null cline makes with the v-axis in Figure 7.14 is given by

$$\theta = \tan^{-1}\left[\frac{w_2 - w_1}{v_2 - v_1}\right]. \tag{7.41}$$

We can now write down very simply a necessary condition for limit cycle oscillations for the piecewise model, that is, conditions for the null clines to be as in Figure 7.14(b). The gradient of the v null cline at the steady state must be less than the gradient, b/γ, of the w null cline; that is,

$$\tan\theta = \frac{w_2 - w_1}{v_2 - v_1} < \frac{b}{\gamma}. \tag{7.42}$$

Sufficient conditions for a limit cycle solution to exist are obtained by applying the results of Section 7.3 and demonstrating that a confined set exists. Analytical expressions for the limits on the applied current I_a for limit cycles can also be found (Exercise 7).

A major property of this model for the space-clamped axon membrane is that it can generate regular beating of a limit cycle nature when the applied current I_a is in an appropriate range $I_1 < I_a < I_2$. The bifurcation to a limit cycle solution when I_a increases past I_1 is essentially a Hopf bifurcation and so the period of the limit cycle is given by an application of the Hopf bifurcation theorem. This model with periodic

beating solutions will be referred to again in Chapter 9 when we consider the effect of perturbations on the oscillations. All of the solution behaviour found with the model (7.39) have also been found in the full Hodgkin–Huxley model, numerically of course. The various solution properties have also been demonstrated experimentally.

Some neuron cells fire with periodic bursts of oscillatory activity like that illustrated in Figures 7.7(b) and (d). We would expect such behaviour if we considered coupled neuronal cells which independently undergo continuous firing. By modifying the above model to incorporate other ions, such as a calcium (Ca^{++}) current, periodic bursting is obtained; see Plant (1978, 1981). There are now several neural phenomena where periodic bursts of firing are observed experimentally. With the knowledge we now have of the qualitative nature of the terms and solution behaviour in the above models and some of their possible modifications, we can now build these into other models to reflect various observations which indicate similar phenomena. The field of neural signalling, both temporal and spatial, is a fascinating and important one which will be an area of active research for many years.

7.6 Modelling the Control of Testosterone Secretion and Chemical Castration

The hormone testosterone, although present in very small quantities in the blood, is an extremely important hormone; any regular imbalance can cause dramatic changes. In man, the blood levels of testosterone can fluctuate periodically with periods of the order of two to three hours. In this section we discuss the physiology of testosterone production and construct and analyse a model, rather different from those we have so far discussed in this chapter, to try and explain the periodic levels of testosterone observed. Although the phenomenon is interesting in its own right, another reason for discussing it is to demonstrate the procedure used to analyse this type of model. Perhaps most important, however, is to try and understand the mechanism of production with a view to aiding current research in controlling testosterone production in its use in (chemical) male contraception and prostate cancer control.

Before describing the important physiological elements in the process of testosterone production, there are some interesting effects and ideas associated with this important hormone. Men have a testosterone level of between 10 to 35 nanomoles per litre of blood, with women having between 0.7 to 2.7 nanomoles per litre. Reduced levels of testosterone, or rather the level of a sex hormone binding globulin (SHBG) directly related to free testosterone, are often accompanied by personality changes—the individual tends to become less forceful and commanding. On the other hand increased levels of testosterone induce the converse. Although the actual differences in testosterone levels are minute, the effects can be major.

In men the high level of testosterone primarily comes from the testes, which produces about 90%, with the rest from other parts of the endocrine system, which is why women also produce it. The drug Goserelin, for example, which was introduced to treat cancer of the prostate, can achieve chemical castration within a few weeks after the start of treatment. The patient's testosterone level is reduced to what would be achieved by removal of the testes. The body does not seem to adjust to the drug and so effective